Supersymmetry Physics at Linear Colliders

Hans-Ulrich Martyn

I. Physikalisches Institut, RWTH Aachen, Germany

The experimental potential of e^+e^- Linear Colliders to explore the properties of supersymmetric particles is reviewed. High precision measurements of masses, spin-parity, gauge quantum numbers, couplings and mixings, production and decay properties will be possible in a clean environment. These achievements will allow the underlying supersymmetry breaking scheme to be revealed, the parameters of the fundamental theory to be determined and to test their unification through extrapolation to very high energie scales.

1 Introduction

There is a worldwide consensus that the next important high energy physics project should be the construction of a e^+e^- Linear Collider (LC) in the $0.5 - 1$ TeV energy range. One of the main arguments is the exploration of supersymmetry (SUSY). If the attractive concept of low energy, electro-weak scale supersymmetry is realised in Nature, then supersymmetry will be discovered at future hadron collider experiments [1, 2]. In many scenarios the production thresholds of the lightest supersymmetric particles, in particular neutralinos and charginos, are expected to be below about 1 TeV, while the LHC is sensitive to gluinos and squarks with masses up to 2.5 TeV. However, the LHC will only be able to reveal the gross features of supersymmetry. Many essential questions will be left open:
— Can each particle be associated to its superpartner with the expected spin-parity, gauge quantum numbers and couplings?
— What are the exact masses, widths and branching ratios? What are the production and decay properties, the mixing parameters and CP phases?
— What is the underlying SUSY breaking mechanism? How to reconstruct the fundamental theory and extrapolate its parameters to high energy, GUT scales?

Answers to these elementary questions can only be provided by precision experiments at a high luminosity e^+e^- Linear Collider. There are currently three Linear Collider projects, well advanced such that their construction may start in the near future: the German TESLA [3] design adopting superconducting cavities, the US NLC [4] and the Japanese JLC [5] projects using normal conducting cavities. The initial energies will be 500 GeV and all LCs will be upgradeable to reach about 1 TeV. This energy may be insufficient to produce the complete sparticle spectrum; ideas for multi-TeV collisions are being developed for CLIC [6]. Some parameters of the future LCs relevant for experimentation are compiled in table 1. Most important for SUSY studies is

Parameter	TESLA		NLC/JLC		CLIC
cms energy [GeV]	500	800	500	1000	3000
accelerating gradient [MV/m]	23.4	35	48	48	150
luminosity L [10^{34}cm^{-2}s^{-1}]	3.4	5.8	2.0	3.4	10
$\mathcal{L}_{int}/10^7$s [fb^{-1}]	340	580	200	340	1000
beamstrahlung spread [%]	3.2	4.3	4.7	10.2	31
beam polarisation	$\mathcal{P}_{e^-}$ = 0.80		$\mathcal{P}_{e^+}$ = 0.60		

Table 1: Some performance parameters of e^+e^- Linear Collider projects

the availability of polarised beams, being indispensable for electrons and highly desirable for positrons. Furthermore e^-e^-, $e^-\gamma$ and $\gamma\gamma$ options may be provided.

The phenomenological implications of several SUSY scenarios, giving very distinct signatures, will be discussed: the minimal supergravity model (mSUGRA), gauge mediated (GMSB) and anomaly mediated (AMSB) supersymmetry breaking models (see e.g. LC reports [3, 4, 5]). Lacking reliable predictions, various benchmark scenarios have been proposed. Extensive work has been done within mSUGRA models, notably assuming the benchmarks of the TESLA TDR [3] and the Snowmass consensus [7].

Simulations of SUSY spectra serve to exploit the potential and to define the requirements of e^+e^- collider experiments; The results can often be easily extrapolated to other model parameters. A general exploration strategy would be to get an overview over the accessible SUSY processes at the highest collider energy and then investigate in a bottom-up approach particular channels choosing the appropriate enegy and beam polarisations. Usually, the background from SUSY is larger than from SM physics.

Obviously the expected accuracy has to be matched with improved, higher order theoretical calculations, as discussed by Majerotto [10]. The extraction of the fundamental SUSY parameters, a model-independent determination of the symmetry breaking mechanism and the extrapolation of these parameters to high scales are discussed by Kalinowski [11].

In the following, studies within mSUGRA are presented, which is characterised by a few parameters: the universal scalar mass m_0, the universal gaugino mass $m_{1/2}$, the trilinear coupling A_0, the ratio of the Higgs vaccum expectation values $\tan\beta$ and the sign of the Higgsino parameter sign μ. Detailed simulations and estimates on precisions achievable in a reasonable run time have been performed for the RR 1 model of the TESLA studies [8, 3] and the Snowmass point SPS 1 [9]. The spectra are shown in fig. 1. Both provide many superpartners to be accessible with a LC of 500 GeV energy, the main differences are τ rich $\tilde{\chi}$ decays of SPS 1 due to the larger $\tan\beta$.

2 Properties of sleptons

Scalar leptons are easy to detect and belong in many models to the lightest observable sparticles. They are produced in pairs

$$e^+e^- \;\rightarrow\; \tilde{\ell}_i^+\tilde{\ell}_j^-,\ \tilde{\nu}_\ell\,\tilde{\nu}_\ell \qquad\qquad [i,j = L,R \text{ or } 1,2] \tag{1}$$

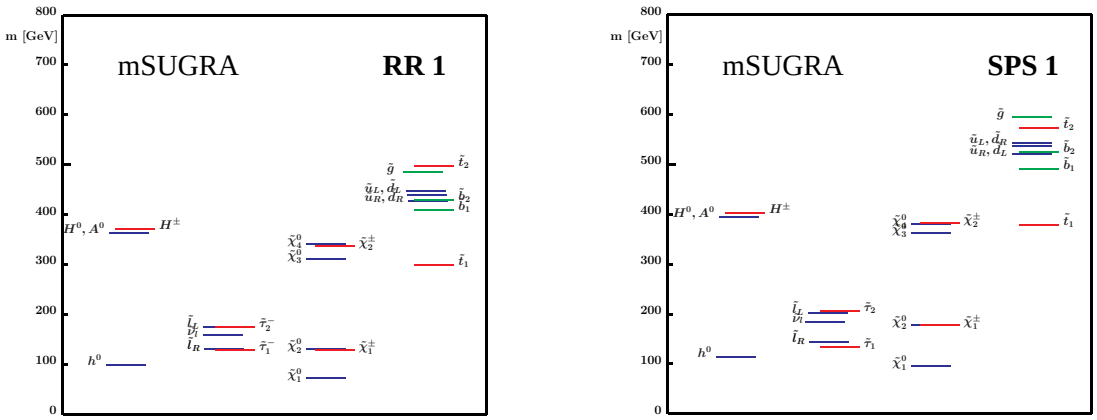

Figure 1: Mass spectra of mSUGRA models RR 1 (parameters $m_0 = 100$ GeV, $m_{1/2} = 200$ GeV, $A_0 = 0$ GeV, $\tan\beta = 3$, sign $\mu +$) and SPS 1 ($m_0 = 100$ GeV, $m_{1/2} = 250$ GeV, $A_0 = -100$ GeV, $\tan\beta = 10$, sign $\mu +$)

via s-channel γ/Z exchange and t-channel $\tilde{\chi}$ exchange for the first generation. The various states and L, R quantum numbers can be efficiently disentangled by a proper choice of beam energy and polarisation. The cross section for $\tilde{\ell}^+_R\tilde{\ell}^-_R$ production is much larger for right-handed e^-_R than for left-handed e^-_L electrons; positron polarisation further enhances the effect.

The isotropic two-body decays

$$\tilde{\ell}^- \rightarrow \ell^-\tilde{\chi}^0_i\,, \tag{2}$$

$$\tilde{\nu}_\ell \rightarrow \ell^-\tilde{\chi}^+_i \tag{3}$$

allow for a clean identification and lead to a uniform lepton energy spectrum. The minimum and maximum ('endpoint') energies

$$E_{+/-} = \frac{m_{\tilde{\ell}}}{2}\left(1 - \frac{m^2_{\tilde{\chi}}}{m^2_{\tilde{\ell}}}\right)\gamma\,(1 \pm \beta) \tag{4}$$

can be used for an accurate determination of the masses of the primary slepton and the secondary neutralino/chargino. This feature makes slepton production particularly attractive.

2.1 Study of smuons in continuum

Examples of mass measurements using the μ energy spectra of $\tilde{\mu}_R\tilde{\mu}_R$ and $\tilde{\mu}_L\tilde{\mu}_L$ production are shown in fig. 2. The distributions are not perfectly flat due to beamstrahlung, QED radiation, selection criteria and detector resolutions. In the simple case of $\tilde{\mu}_R$ pair production a small background from $\tilde{\chi}^0_2\tilde{\chi}^0_1$ is present. With a moderate luminosity the masses $m_{\tilde{\mu}_R}$ and $m_{\tilde{\chi}^0_1}$ can be obtained with an accuracy of about 3 per mil. The partner $\tilde{\mu}_L$ is more difficult to detect because of large background from WW pairs and SUSY cascades. However, with the high luminosity of TESLA one may select the rare decay modes $\tilde{\mu}_L \rightarrow \mu\tilde{\chi}^0_2$ and $\tilde{\chi}^0_2 \rightarrow \ell^+\ell^-\,\tilde{\chi}^0_1$, leading to a unique, background free signature $\mu^+\mu^-\,4\ell^\pm\not{E}$. The contributions of false $\mu^+\mu^-$ pairs from $\tilde{\chi}^0_2$

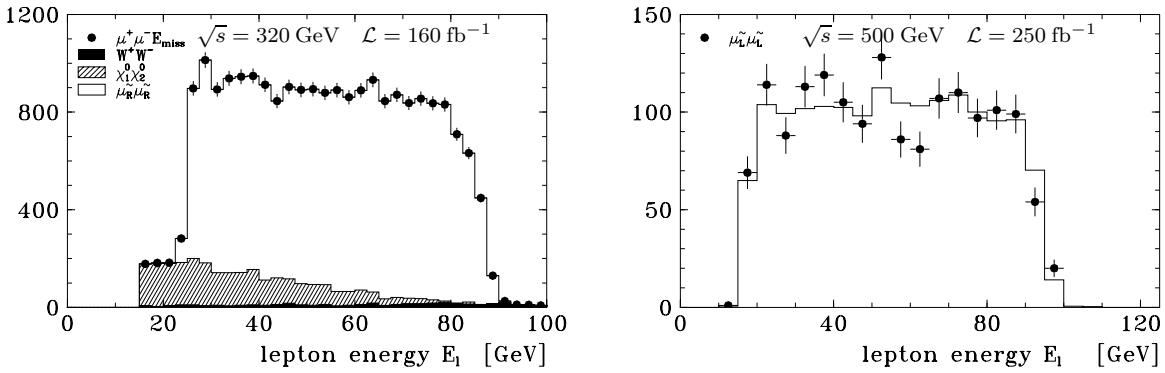

Figure 2: Energy spectra E_μ of muons from the processes $e^-_R e^+_L \to \tilde{\mu}^-_R \tilde{\mu}^+_R \to \mu^- \tilde{\chi}^0_1 \, \mu^+ \tilde{\chi}^0_1$ (left) and $e^-_L e^+_R \to \tilde{\mu}^-_L \tilde{\mu}^+_L \to \mu^- \tilde{\chi}^0_2 \, \mu^+ \tilde{\chi}^0_2$ with $\tilde{\chi}^0_2 \to \ell^+ \ell^- \, \tilde{\chi}^0_1$ (right), assuming mSUGRA model RR 1 [8]

decays can be readily subtracted using the corresponding e^+e^- cascade decays. The achievable mass resolutions for $m_{\tilde{\mu}_L}$ and $m_{\tilde{\chi}^0_2}$ is of the order of 2 per mil.

If the neutralino mass is known one can make use of correlations between the two observed muons. The μ momentum vectors can be arranged with the $\tilde{\chi}^0$ momenta, whose magnitudes are calculable, in such a way as to give two back-to-back primary smuons under the assumption of a kinematically allowed minimum mass $m_{\min}(\tilde{\mu}_R)$. The resulting distribution in fig. 3 has a pronounced edge at the actual smuon mass, while the background is flat. The mass resolution can be improved by a factor of two.

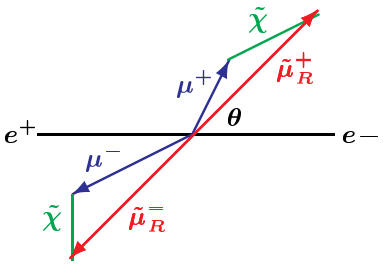

An important quantity is the spin of the slepton which can be directly determined from their angular distribution. If the slepton and neutralino mass are known, one can reconstruct from the event kinematics the polar angle θ of the slepton up to a twofold ambiguity. The wrong solution is flat in $\cos\theta$ and can be subtracted. The angular distribution of the reaction $e^+e^- \to \tilde{\mu}_R \, \tilde{\mu}_R$, shown in fig. 3, clearly exhibits a $\sin^2\theta$ behaviour as expected for a scalar particle.

2.2 Study of selectrons in continuum

Similar investigations can be performed for selectrons, but with higher accuracy due to larger cross sections. Of particular interest is the associated production of

$$e^-_R e^+_R \to \tilde{e}^-_R \tilde{e}^+_L \quad \text{and} \quad e^-_L e^+_L \to \tilde{e}^-_L \tilde{e}^+_R \tag{5}$$

via t-channel $\tilde{\chi}^0$ exchange. Note that both $e^\pm$ beams carry the same helicity, which is 'odd' with respect to the usual γ/Z exchange. For polarised beams the charge of the observed lepton can be directly associated to the L, R quantum numbers of the selectrons and the energy spectrum uniquely determines whether it comes from the $\tilde{e}_R$ or the $\tilde{e}_L$ decay.

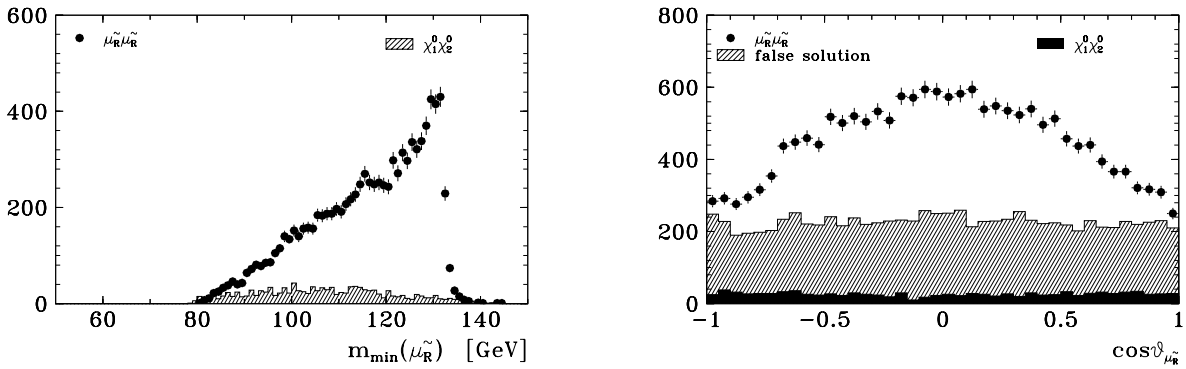

Figure 3: Exploiting momentum correlations in the reaction $e^-_R e^+_L \to \tilde{\mu}^-_R \tilde{\mu}^+_R \to \mu^- \tilde{\chi}^0_1 \, \mu^+ \tilde{\chi}^0_1$, mSUGRA model RR 1 [3]. Minimum mass $m_{\min}(\tilde{\mu}_R)$ (left) and $\tilde{\mu}^+_R$ polar angle distribution (right)

These properties have been used to disentangle the reaction $e^-_{R,L} e^+ \to \tilde{e}_R \tilde{e}_L$ from the simultaneous $\tilde{e}_R \tilde{e}_R$ and $\tilde{e}_L \tilde{e}_L$ production at $\sqrt{s} = 500$ GeV in the SPS 1 scenario [12]. The idea is to eliminate all charge symmetric background by a double subtraction of e^- and e^+ energy spectra and opposite electron beam polarisations $\mathcal{P}_{e^-} = +0.8$ and $\mathcal{P}_{e^-} = -0.8$, symbolically $(E_{e^-} - E_{e^+})_{e^-_R} - (E_{e^-} - E_{e^+})_{e^-_L}$. The results of a simulation, shown in fig. 4, exhibit clear edges or 'endpoints' from the $\tilde{e}_R$ and $\tilde{e}_L$ decays. They can be used to determine both selectron masses to an accuracy of $\delta m_{\tilde{e}_R, \tilde{e}_L} \sim 0.8$ GeV. This elegant method would profit considerably from additional positron beam polarisation, which could effectively enhance the signal and suppress the background.

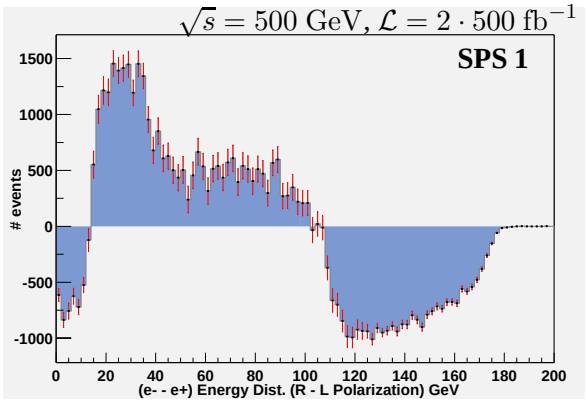

Figure 4: Subtracted energy spectra $(E_{e^-} - E_{e^+})_{e^-_R} - (E_{e^-} - E_{e^+})_{e^-_L}$ of the reaction $e^-_{R,L} e^+ \to \tilde{e}_R \tilde{e}_L$ in mSUGRA model SPS 1 at $\sqrt{s} = 500$ GeV [12]

2.3 Sneutrino production

Sneutrinos are being identified via their decay into the corresponding charged lepton and the subsequent chargino decays $\tilde{\chi}^\pm_1 \to q\bar{q}'/\ell^\pm \nu \, \tilde{\chi}^0_1$ leading to additional jets and leptons. The final topology, e.g. $\tilde{\nu}_\mu \tilde{\nu}_\mu \to \mu^+ \mu^- \ell^\pm 2j \not{E}$ is very clean and the event rates are large, in particular for $\tilde{\nu}_e \tilde{\nu}_e$ production. The energy spectra of the primary leptons, see fig. 5, can be used to determine

$m_{\tilde{\nu}}$ and $m_{\tilde{\chi}_1^\pm}$ to 2 per mil or better. Furthermore the di-jet energy and mass spectra can be used to measure the chargino couplings and the $\tilde{\chi}_1^\pm - \tilde{\chi}_1^0$ mass difference very precisely; a resolution below 50 MeV, given essentially by detector systematics, appears feasible. The detection and measurement of tau-sneutrinos $\tilde{\nu}_\tau$ is more problematic, due to losses in decay modes and decay energy spectra.

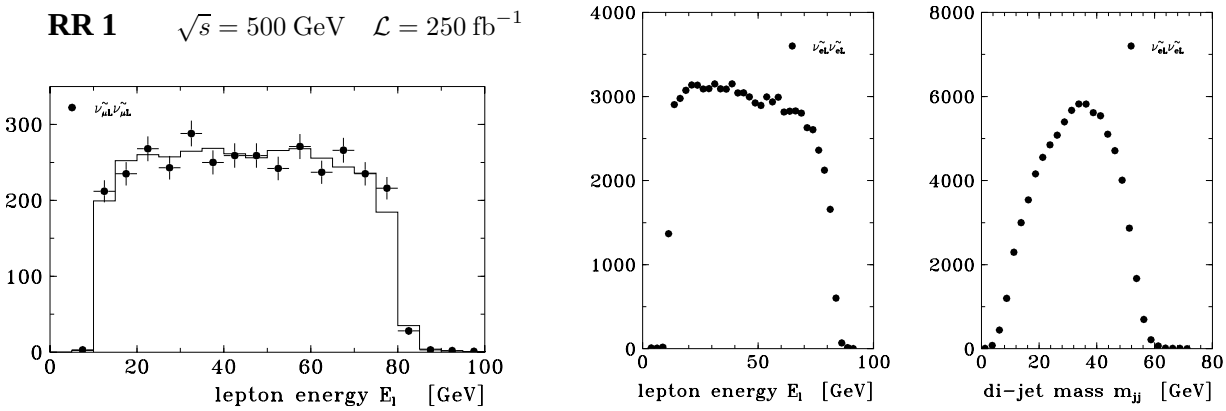

Figure 5: Lepton energy and di-jet mass spectra of $e_L^- e_R^+ \to \tilde{\nu}_\mu \tilde{\nu}_\mu \to \mu^- \tilde{\chi}_1^+ \, \mu^+ \tilde{\chi}_1^-$ (left) and $e_L^- e_R^+ \to \tilde{\nu}_e \tilde{\nu}_e \to e^- \tilde{\chi}_1^+ \, e^+ \tilde{\chi}_1^-$ (center) with subsequent decay $\tilde{\chi}_1^\pm \to q\bar{q}' \, \tilde{\chi}_1^0$ (right) [8, 3]

2.4 Threshold scans

High precision masses of accuracy $\mathcal{O}(0.1 \text{ GeV})$ can be obtained by scanning the excitation curve close to production threshold. Slepton pairs $\tilde{\ell}_i \tilde{\ell}_i$ are produced in a P-wave state with a characteristic rise of the cross section $\sigma_{\tilde{\ell}\tilde{\ell}} \sim \beta^3$, where $\beta = \sqrt{1 - 4\, m_{\tilde{\ell}}^2 / s}$. Thus, a measurement of the shape of the cross section carries information on the mass and the spin $J = 0$ of the sleptons. With the anticipated precision it is necessary to have an improved theory taking the finite width $\Gamma_{\tilde{\ell}}$ and higher order corrections into account. Complete one-loop calculations have been performed for $\tilde{\mu}\tilde{\mu}$ and $\tilde{e}\tilde{e}$ production [13]. Examples of SPS 1 simulations within this frame are shown in fig. 6. Using polarised beams and $\mathcal{L} = 50$ fb^{-1} a (highly correlated) 2-parameter fit gives $\delta m_{\tilde{e}_R} = 0.20$ GeV and $\delta \Gamma_{\tilde{e}_R} = 0.25$ GeV; the resolution deteriorates by a factor of ~ 2 for $\tilde{\mu}_R \tilde{\mu}_R$ production.

A remarkable feature of pure t-channel selectron production, namely $e^+e^- \to \tilde{e}_R \tilde{e}_L$ and $e^-e^- \to \tilde{e}_R \tilde{e}_R, \; \tilde{e}_L \tilde{e}_L$, is that the cross section rises more steeply as $\sigma_{\tilde{e}\tilde{e}} \sim \beta$. This property makes the e^-e^- mode particularly attractive. Moreover, the cross sections are much larger than in e^+e^- collisions, due to the missing destructive interference with the s-channel amplitude. A threshold curve for $e_R^- e_R^- \to \tilde{e}_R \tilde{e}_R$ is shown in fig. 6; the gain in resolution is a factor ~ 4 with only a tenth of the luminosity, compared to e^+e^- beams.

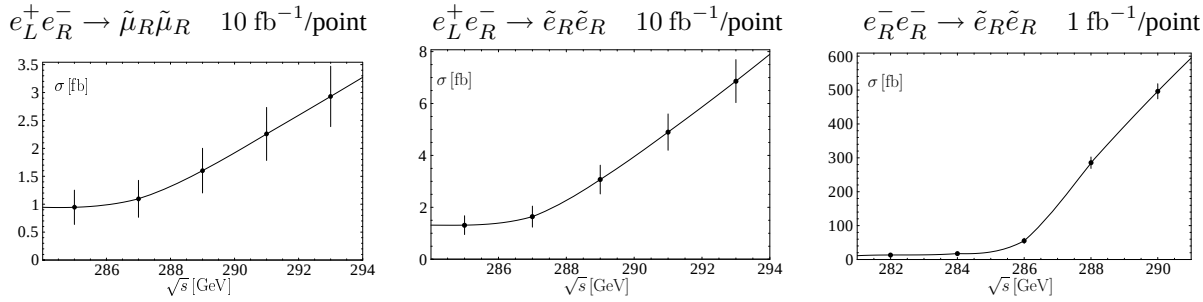

Figure 6: Cross sections at threshold for the reactions $e_L^+e_R^- \to \tilde{\mu}_R\tilde{\mu}_R$, $e_L^+e_R^- \to \tilde{e}_R\tilde{e}_R$ and $e_R^-e_R^- \to \tilde{e}_R\tilde{e}_R$ (SPS 1 scenario) including background [13]. Error bars correspond to a luminosity of $10\ \mathrm{fb}^{-1}$ resp. $1\ \mathrm{fb}^{-1}$ per point

2.5 τ polarisation from $\tilde{\tau}$ decays

Sfermions of the third generation are in general mixed states due to the large Yukawa coupling of their superpartner fermions. For the $\tilde{\tau}$ sector one has

$$\begin{pmatrix} \tilde{\tau}_1 \\ \tilde{\tau}_2 \end{pmatrix} = \begin{pmatrix} \cos\theta_{\tilde{\tau}} & \sin\theta_{\tilde{\tau}} \\ -\sin\theta_{\tilde{\tau}} & \cos\theta_{\tilde{\tau}} \end{pmatrix} \begin{pmatrix} \tilde{\tau}_L \\ \tilde{\tau}_R \end{pmatrix} \tag{6}$$

The mixing angle is related to the off-diagonal elements of the $\tilde{\tau}$ mass matrix

$$\sin 2\theta_{\tilde{\tau}} = \frac{2\, m_\tau\, (A_\tau - \mu\, \tan\beta)}{m^2_{\tilde{\tau}_1} + m^2_{\tilde{\tau}_2}}\,. \tag{7}$$

The detection of $\tilde{\tau}_i \to \tau\tilde{\chi}^0_j$ is more difficult, but offers as additional information the τ polarisation, measurable via the energy spectra of decay particles. This option is useful in order to study neutralino properties and in particular to determine $\tan\beta$ at large values, which is problematic otherwise.

The $\tilde{\tau}$ masses can be determined with the usual techniques of decay spectra (see fig. 7 for $\tau \to \rho\nu$ decay) or threshold scans at the per cent level. The mixing angle $|\cos\theta_{\tilde{\tau}}|$ can be extracted with high accuracy from cross section measurements with different beam polarisations or at different cm energies.

The τ polarisation is related to the mixing of th $\tilde{\tau}$ as well as to the $\tilde{\tau}$ coupling to the neutralino in the decay. The L/R quantum number is not directly transferred to the τ lepton. The gaugino component of $\tilde{\chi}^0$ preserves the 'chirality' flow while the Higgsino causes a flip

$$\tilde{\tau}_{R\,(L)} \to \tau_{R\,(L)}\,\tilde{B} \quad \text{and} \quad \tilde{\tau}_{R\,(L)} \to \tau_{L\,(R)}\,\tilde{H}^0_1\,. \tag{8}$$

The τ polarisation can be measured using the energy distributions of the decay hadrons, e.g. $\tau \to \pi\nu$ and $\tau \to \rho\nu \to \pi^\pm\pi^0\nu$. Very sensitive is the energy ratio $E_{\pi^\pm}/E_\rho$ in ρ decaya, shown in fig. 7 for two opposite maximal polarisations, giving $\delta\mathcal{P}_\tau \lesssim 10\%$. The polarisation can be expressed in terms of the mixing angle $\theta_{\tilde{\tau}}$, $\tan\beta$ and the $\tilde{\chi}^0_1$ components [14]. In a simplified case study an accuracy of 10 per cent for large $\tan\beta$ values was achieved using the τ polarisation.

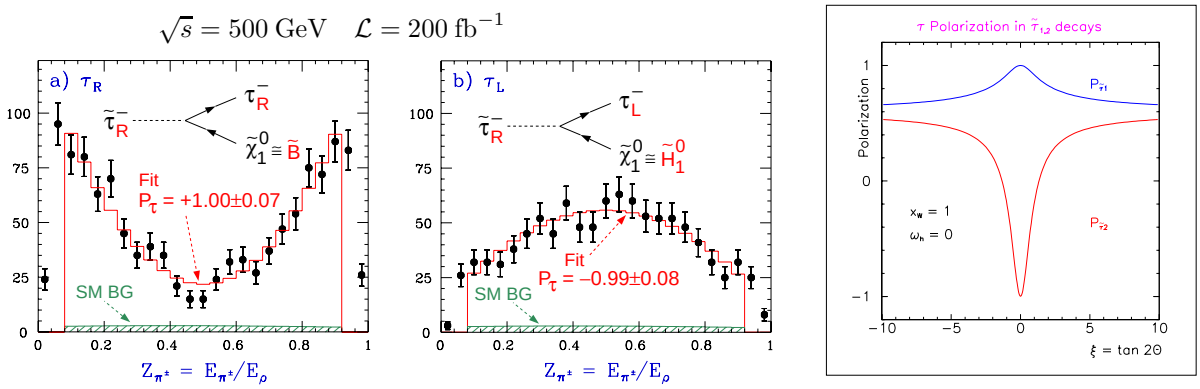

Figure 7: Left: Simulated spectra of $\tau^\pm \to \rho^\pm\nu$ and $\rho^\pm \to \pi^\pm\pi^0$; ratio $E_{\pi^\pm}/E_\rho$ for Bino-like and Higgsino-like $\tilde{\tau}_R\tau\tilde{\chi}_1^0$ couplings [14]. Right: Polarisations $\mathcal{P}_\tau$ of $\tilde{\tau}_1 \to \tau\tilde{\chi}_1^0$ and $\tilde{\tau}_2 \to \tau\tilde{\chi}_1^0$ decays as a function of the $\tilde{\tau}$ mixing angle assuming $\tilde{\chi}_1^0$ to be a pure Bino [15]

The formalism of τ polarisation from $\tilde{\tau}$ decays has been generalised for any choice of MSSM parameters [15]. Fig. 7 shows the polarisation dependence on the mixing angle for a $\tilde{\chi}_1^0$ being a pure Bino. For small mixings both $\tilde{\tau}$'s behave very different. However, in order to be useful for a precise evaluation of large values of $\tan\beta$, the decay neutralinos must have a considerable Higgsino component. Assuming that the parameters of the neutralino sector are well measured elsewhere (see section 3.3), the application of eq. (7) would give direct access to the trilinear A_τ coupling.

2.6 Testing SUSY relations in slepton sector

The precise measurements of slepton properties can be used to extract the underlying SUSY parameters m_0, $m_{1/2}$ and $\tan\beta$ and to perform stringent tests of basic relations in the slepton sector. These results may then be compared to the findings in the chargino and neutralino systems.

- Supersymmetry requires the SM gauge couplings $g(Vff)$ and $\bar{g}(V\tilde{f}\tilde{f})$ of a vector boson V and the Yukawa coupling $\hat{g}(\tilde{V}f\tilde{f})$ of the corresponding gaugino $\tilde{V}$ to be identical, $g = \bar{g} = \hat{g}$. The couplings can be extracted from cross section measurements and their equality can be checked within a fraction of per cent.

- The universality and flavour dependence of slepton masses can be checked at the per mil level.

- The superpartner $\tilde{\nu}_R$ of right handed neutrinos would change the slepton mass predictions and may become observable via $2\,(m^2_{\tilde{\nu}_R} - m^2_{\tilde{\nu}_\tau}) \approx m^2_{\tilde{e}_R} - m^2_{\tilde{\tau}_1}$, valid up to higher orders [19].

- The robust tree-level prediction $m^2_{\tilde{\ell}_L} - m^2_{\tilde{\nu}_\ell} = -m^2_W \cos 2\,\beta$ relates the L-slepton masses of one generation and can be tested very accurately. It further offers a model-independent determination of low values of $\tan\beta$.

3 Properties of charginos and neutralinos

Charginos and neutralinos are produced in pairs

$$e^+e^- \rightarrow \tilde{\chi}_i^+\tilde{\chi}_j^- \qquad [i,j=1,2] \tag{9}$$
$$\rightarrow \tilde{\chi}_i^0\tilde{\chi}_j^0 \qquad [i,j=1,\ldots,4] \tag{10}$$

via s-channel γ/Z exchange and t-channel $\tilde{e}$ or $\tilde{\nu}_e$ exchange. Beam polarisations are important to study the $\tilde{\chi}$ properties and couplings, e.g. by manipulating the $\tilde{\nu}_e$ exchange contribution. Since charginos and neutralinos carry spin $1/2$, the cross section rises as $\sigma_{\tilde{\chi}\tilde{\chi}} \sim \beta$ leading to steep excitation curves at threshold.

Charginos and neutralinos decay into their lighter partners and gauge or Higgs bosons and sfermion-fermion pairs. For the light $\tilde{\chi}$ states, only three-body decays via virtual gauge bosons and sfermions may be kinematically possible

$$\tilde{\chi}_i \rightarrow Z/W\,\tilde{\chi}_j,\ h\,\tilde{\chi}_j \tag{11}$$
$$\tilde{\chi}_1^+ \rightarrow \tilde{\ell}^+\nu_\ell \rightarrow \ell^+\nu_\ell\,\tilde{\chi}_1^0 \tag{12}$$
$$\rightarrow \ell^+\tilde{\nu}_\ell\,\tilde{\chi}_1^0,\ q\bar{q}'\,\tilde{\chi}_1^0 \tag{13}$$
$$\tilde{\chi}_2^0 \rightarrow \tilde{\ell}\ell \rightarrow \ell\ell\,\tilde{\chi}_1^0 \tag{14}$$
$$\rightarrow \ell\ell\,\tilde{\chi}_1^0, q\bar{q}\,\tilde{\chi}_1^0 \tag{15}$$

In MSSM scenarios with R-parity conservation the lightest neutralino $\tilde{\chi}_1^0$ is stable. The signatures are multi-lepton, multi-jet final states with large missing energy. Similar to the slepton analyses, the energy and mass spectra of di-leptons respectively di-jets give access to accurate determinations of the primary and secondary $\tilde{\chi}$ masses and mass differences.

3.1 Chargino studies

Chargino production occurs at a fairly large rate. Results of a simulation of the reaction $e^+_Re^-_L \rightarrow \tilde{\chi}_1^+\tilde{\chi}_1^- \rightarrow \ell^\pm\nu_\ell\tilde{\chi}_1^0\,q\bar{q}'\tilde{\chi}_1^0$ are presented in fig. 8. From the di-jet energy distribution one expects a mass resolution of $\delta m_{\tilde{\chi}_1^\pm} = 0.2\ \mathrm{GeV}$, while the di-jet mass distributions constrains the $\tilde{\chi}_1^\pm - \tilde{\chi}_1^0$ mass splitting within about $100\ \mathrm{MeV}$. The excitation curve clearly exhibits the β dependence consistent with the spin $J = 1/2$ hypothesis. The mass resolution is excellent of $\mathcal{O}(50\ \mathrm{MeV})$, degrading to the per mil level for the higher $\tilde{\chi}_2^\pm$ state.

The properties of $\tilde{\chi}^\pm$ system also depend on the exchanged sneutrino which may be too heavy to be produced directly at the LC. High sensitivity to the $\tilde{\nu}_e$ mass can be reached by studying polarised cross sections and spin correlations between the beam electron and the lepton in the decay $\tilde{\chi}_1^- \rightarrow e^-\,\nu_e\,\tilde{\chi}_1^0$, as shown in fig. 9. From such measurements one may indirectly detect sneutrinos up to masses of 1 TeV with a precision of 10 GeV.

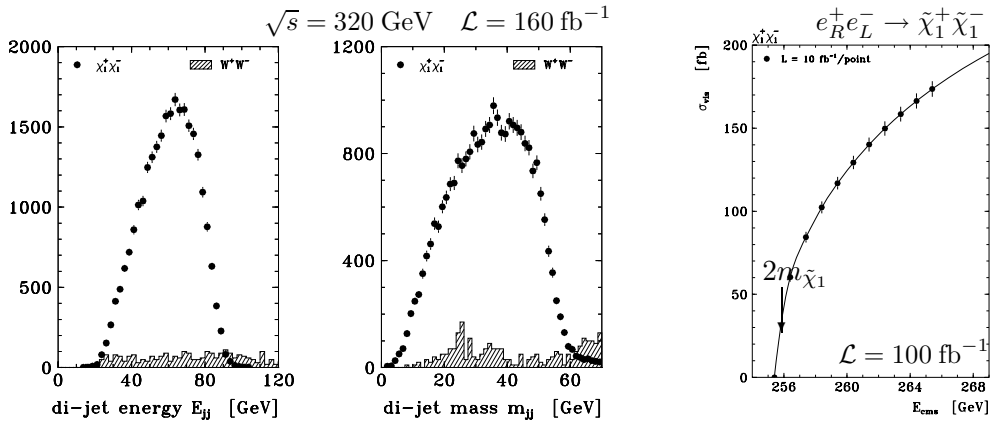

Figure 8: Distributions of $e_R^+e_L^- \to \tilde{\chi}_1^+\tilde{\chi}_1^- \to \ell^\pm\nu_\ell\tilde{\chi}_1^0\, q\bar{q}'\tilde{\chi}_1^0$ in the RR 1 scenario [8, 3]. Left: Di-jet energy and di-jet mass. Right: Cross section at threshold with errors corresponding to 10 fb^{-1} per point.

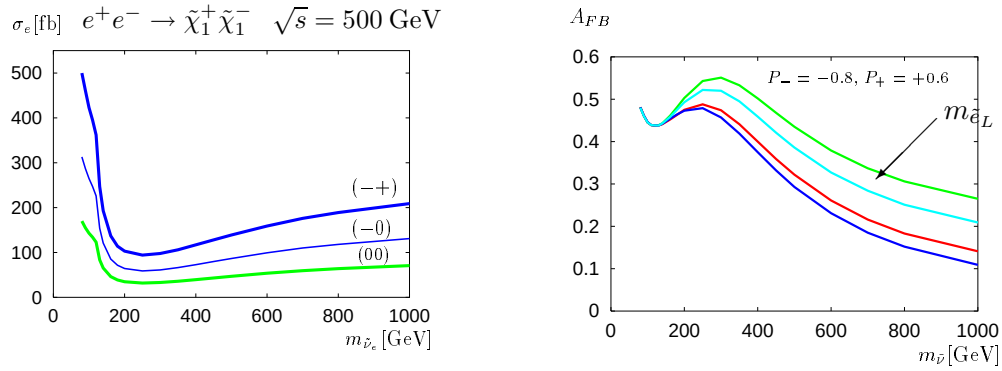

Figure 9: Polarised cross sections for $e^+e^- \to \tilde{\chi}_1^+\tilde{\chi}_1^-$ as a function of $\tilde{\nu}_e$ mass (left) and e^- forward-backward asymmetry of the decay $\tilde{\chi}_1^- \to e^-\,\nu_e\,\tilde{\chi}_1^0$ for various selectron masses rising as indicated by the arrow (right) [3]

3.2 Neutralino studies

The lightest detectable neutralino system $\tilde{\chi}_1^0\tilde{\chi}_2^0$ is difficult to observe in the presence of other SUSY particle production. More suitable is the reaction $e^+e^- \to \tilde{\chi}_2^0\tilde{\chi}_2^0 \to 2(\ell^+\ell^-)\,\tilde{\chi}_1^0\tilde{\chi}_1^0 \to 4\ell^\pm\not{E}$with $\ell = e,\ \mu$. Again the di-lepton energy and mass distributions can be used to determine the neutralino masses. The problem of wrong lepton pairing can be readily solved by subtracting the false $e\,\mu$ combinations. From the spectra presented in fig. 10 one expects uncertainties in the primary and secondary $\tilde{\chi}_2^0$ and $\tilde{\chi}_1^0$ masses of about 2 per mil. Note that the mass difference $\Delta m_{\tilde{\chi}_2^0-\tilde{\chi}_1^0}$ can be determined very precisely using the abundant cascade decays of other SUSY particles. A more accurate mass of $\delta m_{\tilde{\chi}_2^0} < \mathcal{O}(100\,\mathrm{MeV})$ can be derived from a threshold scan. The higher mass $\tilde{\chi}_3^0$ and $\tilde{\chi}_4^0$ states, if accessible, can still be resolved with a resolution of a few hundred MeV.

Similar to the chargino system, the study of polarised cross section and spin correlations in angular distributions of $\tilde{\chi}_2^0 \to \ell^+\ell^-\tilde{\chi}_1^0$ decays provide high sensitivity to the exchanged selectron and the gaugino parameter M_1, which is complementary to $\tilde{e}\tilde{e}$ production.

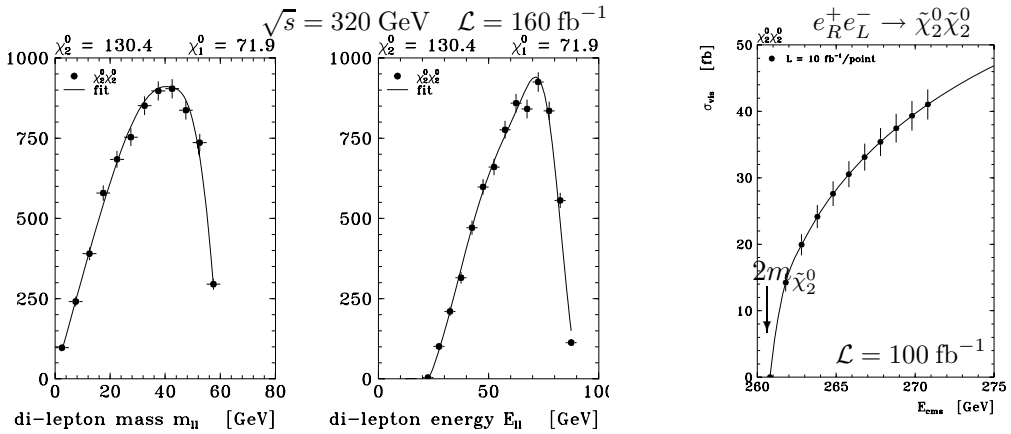

Figure 10: Distributions of $e^+e^- \to \tilde{\chi}_2^0\tilde{\chi}_2^0 \to 4\,\ell^\pm\,\tilde{\chi}_1^0\tilde{\chi}_1^0$, scenario RR 1 [8, 3]. Left: Di-lepton mass and di-lepton energy. Right: Cross section at threshold with errors corresponding to 10 fb^{-1} per point.

3.3 Chargino and neutralino systems

The chargino system can be described by the fundamental MSSM parameters M_2, μ and $\tan\beta$. The neutralino sector depends in addition to these parameters on the $U(1)$ gaugino mass M_1. From the multitude of precision measurements — masses, polarised cross sections, polarisation asymmetries, etc. — it is possible to construct an over-constrained set of SUSY relations and to derive the basic parameters including all mixings in a model-independent way [16, 17]. Applied to the RR 1 benchmark point one finds $M_1 = 78.7 \pm 0.7$ GeV, $M_2 = 152 \pm 1.8$ GeV, $\mu = 316 \pm 0.9$ GeV and $\tan\beta = 3 \pm 0.7$. However, this procedure has poor or almost no sensitivity to large values of $\tan\beta$. In this case additional information may be provided by the τ polarisation in the $\tilde{\tau}$ system (see section 2.5).

In general the parameters M_1 and μ may be complex, allowing for $\mathcal{CP}$ violating phases. This can be taken into account in such an analysis [17], although the sensitivity to masses and cross sections is rather limited. It is certainly more sensible to look directly for $\mathcal{CP}$ sensitive observables, like triple vector products, in the chargino/neutralino systems.

4 Stop quark studies

It is conceivable that the lightest superpartner of the quarks is the stop quark $\tilde{t}$ due to substantial mixings between $\tilde{t}_R$ and $\tilde{t}_L$ induced by the large Yukawa coupling to the top mass. The $\tilde{t}$ quark phenomenology is completely analogous to that of the $\tilde{\tau}$ system. It is characterised by two mass eigenstates st_1 and $\tilde{t}_2$ and a mixing angle $\theta_{\tilde{t}}$, the lighter state being $\tilde{t}_1 = \tilde{t}_L \cos\theta_{\tilde{t}} + \tilde{t}_R \sin\theta_{\tilde{t}}$. If the mass $m_{\tilde{t}_1}$ is below 250 GeV, it may not be observed at LHC and it may be discovered at the Linear Collider.

The production of $e^+e^- \to \tilde{t}_1\tilde{t}_1$ has been studied for typical decay modes $\tilde{t}_1 \to c\,\tilde{\chi}_1^0$ and $\tilde{t}_1 \to b\,\tilde{\chi}_1^\pm$. Both the mass and mixing angle can be determined simultaneously by measuring the production cross section with different beam polarisations, e.g. $\sigma_{e_R^-e_L^+}$ and $\sigma_{e_L^-e_R^+}$. Th results of a high luminosity simulation [18], presented in the $m_{\tilde{t}_1} - \cos\theta_{\tilde{t}}$ plane of fig. 11, provide high accuracies on the mass and mixing angle.

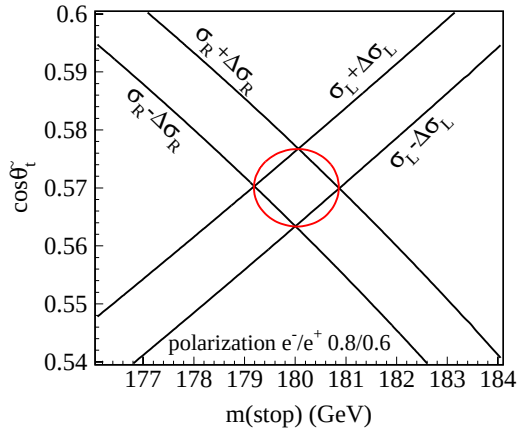

Figure 11: Contours of $\sigma_{RL}(\tilde{t}_1\tilde{t}_1)$ and $\sigma_{LR}(\tilde{t}_1\tilde{t}_1)$, $\tilde{t}_1(180) \to b\,\tilde{\chi}_1^{\pm}(150)$ as a function of $m_{\tilde{t}_1}$ and $\cos\theta_{\tilde{t}}$ for $\sqrt{s} = 500$ GeV, $\mathcal{L} = 2 \cdot 500\ \mathrm{fb}^{-1}$ [18]

5 A run scenario to explore mSUGRA

One may wonder if such a rich programme, i.e. exploiting the properties of all kinematically accessible sparticles through cross section measurements in the continuum and at threshold including various combinations of beam polarisations, can be performed in a reasonable time. At the *Snowmass Summer Study 2001* a possible run scenario for the SPS 1 mSUGRA benchmark model has been constructed [9]. The NLC machine performance was assumed with an energy of $\sqrt{s} = 500$ GeV and an electron (no positron) beam polarisation of $\mathcal{P}_{e^-} = 0.8$. The task was to distribute an integrated luminosity of $\mathcal{L} = 1000\ \mathrm{fb}^{-1}$ (500 GeV equivalent) and to estimate the achievable precisions on the SUSY mass spectrum. The time needed to accumulate the data corresponds to four good years of NLC operation or probably rather seven years including the start up phase.

	$\sqrt{s}$	$\mathcal{P}_{e^-}$	$\mathcal{L}$ [fb^{-1}]	Comments
e^+e^-	500	L/R	335	max. energy
e^+e^-	270	L/R	100	$\tilde{\chi}_1^0\tilde{\chi}_2^0$ (L)
				$\tilde{\tau}_1\tilde{\tau}_1$ (R)
e^+e^-	285	R	50	$\tilde{\mu}_R\tilde{\mu}_R$, $\tilde{e}_R\tilde{e}_R$
e^+e^-	350	L/R	40	$t\bar{t}$
				$\tilde{e}_R\tilde{e}_L$ (L & R)
				$\tilde{\chi}_1^+\tilde{\chi}_1^-$ (L)
e^+e^-	410	L	100	$\tilde{\tau}_2\tilde{\tau}_2$
				$\tilde{\mu}_L\tilde{\mu}_L$
e^+e^-	580	L/R	90	$\tilde{\chi}_1^{\pm}\tilde{\chi}_2^{\mp}$
e^-e^-	285	RR	10	$\tilde{e}_R\tilde{e}_R$

Table 2: A run scenario for the SPS 1 mSUGRA model [9]. Allocated energy, beam polarisation and luminosity and achievable mass precisions

	m [GeV]	δm_{c}	δm_{s}	δm_{SPS1}
$\tilde{e}_R$	143	0.19	0.02	0.02
$\tilde{e}_L$	202	0.27	0.30	0.20
$\tilde{\mu}_R$	143	0.08	0.13	0.07
$\tilde{\mu}_L$	202	0.70	0.76	0.51
$\tilde{\tau}_1$	135	1 - 2	0.64	0.64
$\tilde{\tau}_2$	206	–	0.86	0.86
$\tilde{\nu}_e$	186	0.23	–	0.23
$\tilde{\nu}_\mu$	186	7.0	–	7.0
$\tilde{\nu}_\tau$	185	–	–	–
$\tilde{\chi}_1^0$	96	0.07	–	0.07
$\tilde{\chi}_2^0$	175	1 - 2	0.12	0.12
$\tilde{\chi}_3^0$	343	8.5	–	8.5
$\tilde{\chi}_4^0$	364	–	–	–
$\tilde{\chi}_1^{\pm}$	175	0.19	0.18	0.13
$\tilde{\chi}_2^{\pm}$	364	4.1	–	4.1

The results of this study are compiled in table 2. For all sparticles, except the muon and tau sneutrinos and the heavy $\tilde{\chi}$ states, mass resolutions of a few hundred MeV or better have been

estimated. Under the assumption that mSUGRA is the correct underlying theory, the SUSY parameters can be deduced with high precision: $m_0 = 100 \pm 0.08$ GeV, $m_{1/2} = 250 \pm 0.20$ GeV, $A_0 = 0 \pm 13$ GeV and $\tan\beta = 10 \pm 0.5$.

Similar precisions are quoted in a study of the RR 1 model at the TESLA LC [8], where one profits from higher rates due to the availability of polarised positrons.

6 R-parity violation

Many supersymmetric models assume that R-parity, $R_p = (-1)^{3B+L+2S}$, is a conserved quantity. There is, however, no strong theoretical argument for this assumption. The general superpotential contains $\not{R}_p$ tri-linear terms which violate lepton-number and baryon-number

$$W_{\not{R}_p} = \underbrace{\lambda_{ijk} L_i L_j \bar{E}_k}_{\delta L \neq 0} + \underbrace{\lambda'_{ijk} L_i Q_j \bar{D}_k}_{\delta L \neq 0} + \underbrace{\lambda''_{ijk} \bar{U}_i \bar{D}_j \bar{D}_k}_{\delta B \neq 0} . \tag{16}$$

R_p violation changes the SUSY phenomenology drastically. The lightest superpartner (LSP), usually the neutralino $\tilde{\chi}^0_1$, is no longer stable. Instead of the typical missing energy signature there are characteristic multi-lepton, multi-jet final states. A systematic investigation of $e^+e^- \to \tilde{\chi}^+_1\tilde{\chi}^-_1$, $\tilde{\chi}^0_i\tilde{\chi}^0_j$ production [20] demonstrates that $\not{R}_p$ decays are easily recognised as events with at least three leptons plus few missing energy or jets (λ or λ' couplings) or multi-jet events (6-10 jets for $\lambda'' > 0$). Despite large combinatorics a $\tilde{\chi}^0_1$ mass reconstruction appears feasible.

For not too small $\not{R}_p$ couplings λ_{1j1} single sparticle production $e^+e^- \to \tilde{\nu} \to \ell\bar{\ell}$, $\ell^\pm\tilde{\chi}^\mp_j$ is possible, to be significantly enhanced by $e^+_L e^-_L$ or $e^+_R e^-_R$ beam polarisations. The reaction

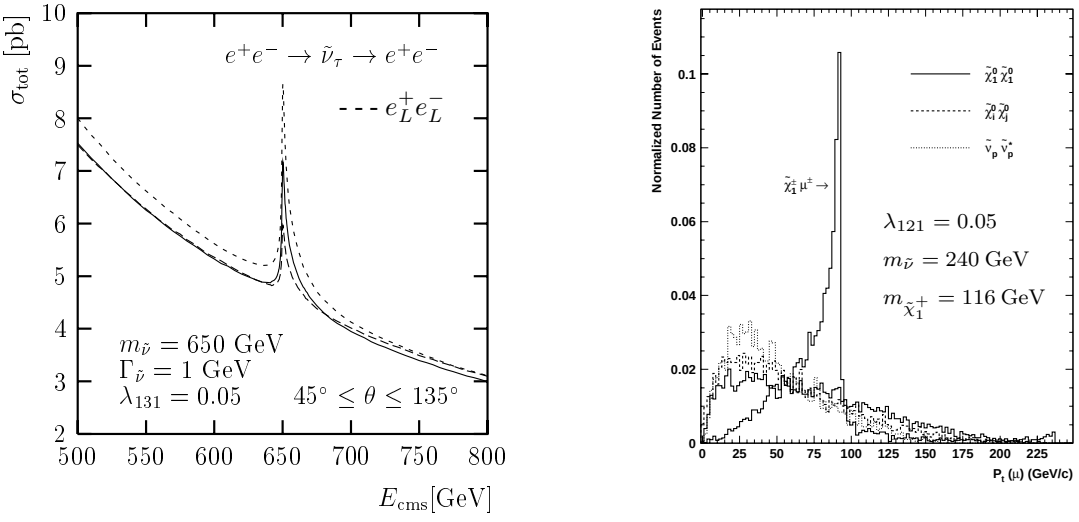

Figure 12: $\not{R}_p$ signals in resonance production $e^+e^- \to \tilde{\nu}_\tau \to e^+e^-$ interfering with Bhabha scattering (left) and muon $p^\mu_\perp$ spectrum in $e^+e^- \to \tilde{\chi}^\pm_1\mu^\mp$ with $\tilde{\chi}^\pm_1 \to \ell^\pm\nu_\ell\,\tilde{\chi}^0_1$, $\tilde{\chi}^0_1 \to ee\nu_\mu$, $\mu e\nu_e$ at $\sqrt{s} = 500$ GeV (right), from ref. [3]

$e^+e^- \to \tilde{\nu} \to e^+e^-$, interfering with Bhabha scattering, is particular interesting, as illustrated in fig. 12. For $m_{\tilde{\nu}} < \sqrt{s}$ one expects spectacular narrow resonances, while very heavy sneutrinos can be detected via contact interactions up to $m_{\tilde{\nu}} = 1.8$ TeV for $\lambda_{1j1} = 0.1$ at the highest LC energy.

A simulation of single chargino production $e^+e^- \to \mu^\mp \tilde{\chi}_1 \to \mu^\mp 3\,\ell \not{E}$ is presented in fig. 12. The process can be easily identified and the pronounced peak of the recoil muon momentum can be used to measure the $\tilde{\chi}_1^\pm$ mass very accurately. A sensitivity of $\lambda_{121} = 10^{-4}$ for masses $m_{\tilde{\nu}} \simeq 150{-}600\,\mathrm{GeV}$ can be reached at $\sqrt{s} = 500\,\mathrm{GeV}$. An interesting aspect is the polarisation dependence, $e^+_L e^-_L \to \tilde{\chi}_1^- \mu^+$ and $e^+_R e^-_R \to \tilde{\chi}_1^+ \mu^-$, caused by helicity flip of the λ_{121} coupling.

7 AMSB scenario

In anomaly mediated SUSY breaking, AMSB, the symmetry breaking is not directly communicated, but is caused by loop effects. The gaugino and scalar masses are dynamically generated via loops. A characteristic feature is that gaugino masses are no longer universal and are related by the reversed hierarchy $M_1 \simeq 2.8\,M_2$ at the electroweak scale. Now the wino is the lightest supersymmetric particle, which leads to almost degenerate masses of the light chargino $\tilde{\chi}_1^\pm$ and the wino-like neutralino $\tilde{\chi}_1^0$.

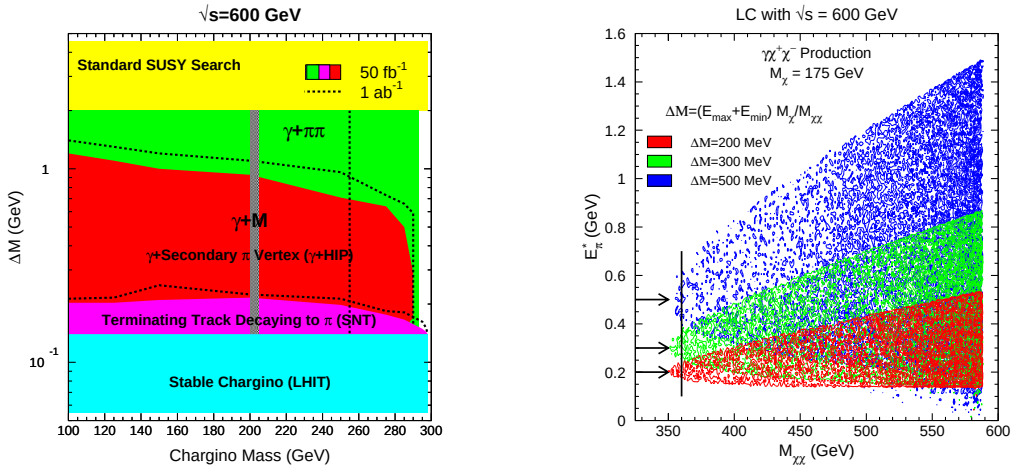

Figure 13: LC potential at $\sqrt{s} = 600$ GeV to search for $e^+e^- \to \tilde{\chi}_1^+\tilde{\chi}_1^-\,(\gamma)$ in AMSB scenarios [21]. Discovery modes and reach as function of $\Delta m_{\tilde{\chi}_1}$ and $m_{\tilde{\chi}_1^\pm}$ (left) and distributions E_π versus $m_{\tilde{\chi}\tilde{\chi}}$ in $\tilde{\chi}\tilde{\chi}$ system of the decay $\tilde{\chi}_1^\pm \to \pi^\pm \tilde{\chi}_1^0$ (right)

The decay modes and lifetime, and hence the search strategy for $e^+e^- \to \tilde{\chi}_1^+\tilde{\chi}_1^-(\gamma)$ [21], depend entirely on the small mass difference $\Delta m_{\tilde{\chi}_1} = m_{\tilde{\chi}_1^\pm} - m_{\tilde{\chi}_1^0}$, typically in the range $0.2 - 2$ GeV. Background from $e^+e^- \to e^+e^-\pi\pi$ can be effectively suppressed by tagging an additional photon. The signatures comprise a stable heavily ionising chargino, a chargino decaying inside the detector with or without visible secondary particles, low momentum pions associated to secondary vertices and standard topologies. The LC discovery potential for AMSB scenarios is shown in fig. 13. Large parts of the $\Delta m_{\tilde{\chi}_1} - m_{\tilde{\chi}_1^\pm}$ region are covered up

to masses close to the kinematic production limit already with a low luminosity of $50\ \mathrm{fb}^{-1}$. A measurement of the pion energy in the decay $\tilde{\chi}_1^{\pm} \to \pi^{\pm}\tilde{\chi}_1^0$ allows for a very precise determination of the mass difference $\Delta m_{\tilde{\chi}_1}$. The $\tilde{\chi}_1$ masses can be reconstructed to an accuracy of order one GeV from the energy spectrum of the radiative photon.

The full exploration of AMSB spectra, exhibiting substantially different properties compared to other SUSY breaking scenarios, and the extraction of the fundamental parameters (m_0, $m_{3/2}$, $\tan\beta$, $\mathrm{sign}\,\mu$) follows along the same lines as discussed above.

8 GMSB scenario

Supersymmetry breaking may also occur at a lower scale $\sqrt{F} \sim \mathcal{O}(100\ \mathrm{TeV})$, much below supergravity, and gauge interactions may serve as messengers, a mechanism called gauge mediated SUSY breaking GMSB. The spectra of GMSB models have charginos, neutralinos and sleptons much lighter than squarks and gluinos. Most characteristic, the LSP is a light gravitino $\tilde{G}$ of mass $m_{\tilde{G}} \simeq (\sqrt{F}/100\ \mathrm{TeV})^2\ \mathrm{eV}$. The phenomenology is determined by the properties of the next lightest sparticle, the unstable NLSP $\tilde{\chi}_1^0$, $\tilde{\tau}_1$ or $\tilde{e}_R$, which decays into the gravitino with a lifetime $c\,\tau \propto (\sqrt{F})^4/(m_{\mathrm{NLSP}})^5$. The theoretically allowed range of scales $\sqrt{F}$ translates into expected NLSP decay lengths of $10^{-4} - 10^5\ \mathrm{cm}$. Conversely, the detection of a NLSP decay and a measurement of its lifetime can be used to pin down the GMSB scenario and to extract the fundamental symmetry breaking scale.

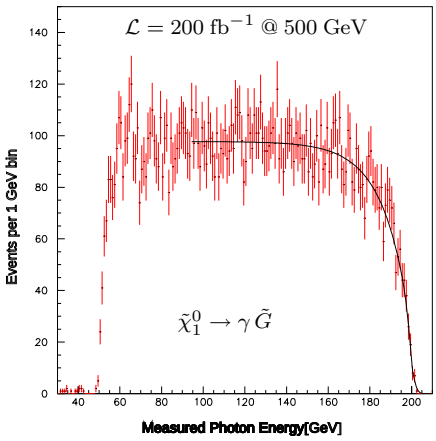

Figure 14: Simulated photon energy spectrum E_γ of the reaction $e^+e^- \to \tilde{\chi}_1^0\tilde{\chi}_1^0$ with $\tilde{\chi}_1^0 \to \gamma\tilde{G}$ in a GMSB scenario, assuming $\mathcal{L} = 200\ \mathrm{fb}^{-1}$ at $\sqrt{s} = 500\ \mathrm{GeV}$, The curve represents a fit to $m_{\tilde{\chi}_1^0} = 197.3 \pm 0.3\ \mathrm{GeV}$ [22]

Detailed studies over a large GMSB parameter space are presented in ref. [22] including simulations of inclusive $\tilde{\chi}_1^0$ (NLSP) production and assuming the detector design of the TESLA TDR. Experimental signatures of the decays $\tilde{\chi}_1^0 \to \gamma\tilde{G},\ f\bar{f}\tilde{G}$ are displaced and time delayed photons and secondary vertices. The photon energy spectrum of the reaction $e^+e^- \to \tilde{\chi}_1^0\tilde{\chi}_1^0 \to \gamma\gamma\,\tilde{G}\tilde{G}$, shown in fig. 14, provides the neutralino mass within two per mil. Various techniques like pointing calorimetry, tracking, vertexing and statistical photon counting methods ensure a measurement of the NLSP decay length $c\tau$ to better than 10% over a large range of $30\,\mu\mathrm{m} - 40\,\mathrm{m}$. This provides a precision below 5% on the symmetry breaking scale over the entire interesting region $\sqrt{F} = 1 - 10^4\ \mathrm{TeV}$.

Scenarios with sleptons as NLSP, e.g. decays $\tilde{\tau}_1 \rightarrow \tau\tilde{G}$ leading to long lived, heavy particles or τ pairs from secondary vertices, have also been investigated [22]. NLSP lifetime and mass measurements of the accessible sparticle spectrum can be used to determine the fundamental GMSB parameters ($M_{\rm mess}$, $N_{\rm mess}$, Λ, $\tan\beta$, sign μ) at the per cent level or better.

9 Experimentation at CLIC

A multi-TeV collider like CLIC may be required to explore the complete spectrum of SUSY particles. In particular the coloured squarks and gluinos are in many models expected to be very heavy, with masses of order TeV. Experimental challenges at these high energies are the low cross sections, the diminishing mass differences within a sparticle multiplet, the cm energy smearing due to increasing QED radiation and beamstrahlung (see table 1) and a reduced resolution of high momentum particles.

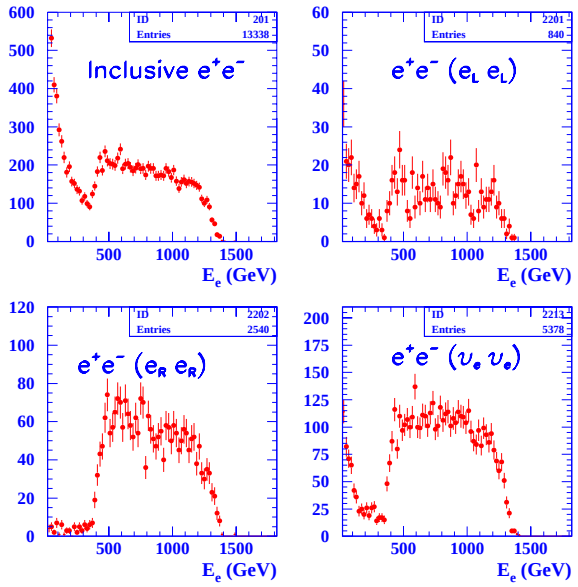

Figure 15: Inclusive $e^{\pm}$ energy spectra of di-electron events with contributions from $e^+e^- \rightarrow \tilde{e}_L\tilde{e}_L$, $\tilde{e}_R\tilde{e}_R$ and $\tilde{\nu}_e\tilde{\nu}_e$ production, for SPS 2 model. Simulation of CLIC conditions assuming $\sqrt{s} = 3.5$ TeV and $\mathcal{L} = 650\ \mathrm{fb}^{-1}$, ref. [23]

A first case study has been performed for $e^+e^- \rightarrow \tilde{e}_R\tilde{e}_R$, $\tilde{e}_L\tilde{e}_L$ and $\tilde{\nu}_e\tilde{\nu}_e$ production in the focus point mSUGRA scenario SPS 2 [23]. In this model the sleptons are relatively heavy with masses ~ 1.45 TeV and widths of order 10 GeV comparable to the mass separation, while the $\tilde{\chi}$ states are much lighter ($100 - 300$ GeV), thus opening many decay channels. Simulations of energy spectra of di-electron events are shown in fig. 15 for $\sqrt{s} = 3.5$ TeV. Energy 'endpoints' are clearly observable. However, all sparticles provide very similar spectra and are difficult to resolve. Beam polarisation and further topology information may help to disentangle the selectrons and e-sneutrino. The detection and study of squarks, smuons and staus is much more difficult, the production rates being an order of magnitude smaller.

At high masses the excitation curves are less steep and their rise extends over few hundred GeV, possibly covering several production thresholds. An anticipated precision at the per cent level requires good knowledge of the branching ratios and control of the background to atto-barns.

Obviously, a comprehensive study of very heavy sparticles is an ambitious task. It appears to be feasible with the present CLIC design, although with less accuracy than for lower mass states. In any case high luminosity and high beam polarisations are mandatory, a reduction of the beamstrahlung width would be desirable.

10 Conclusions and outlook

Experiments at future e^+e^- Linear Colliders offer an enormous potential to discover and explore the superparticle spectra and will be essential to establish the basic concepts of supersymmetry. Linear Colliders are ideal instruments to carry out extremely precise measurements of the superpartner properties and interactions. Specifically such measurements comprise masses, widths, branching ratios, couplings and mixing parameters, gauge quantum numbers, spin-parity, $\mathcal{CP}$ phases, ... These high precision data are necessary in order to perform model independent analyses of the detailed structure of the underlying supersymmetry theory, to determine its fundamental parameters and the symmetry breaking mechanism. The resulting reliable extrapolations to very high scales offer the possibility to test our ideas on particle physics close to the Planck scale, where gravity becomes important.

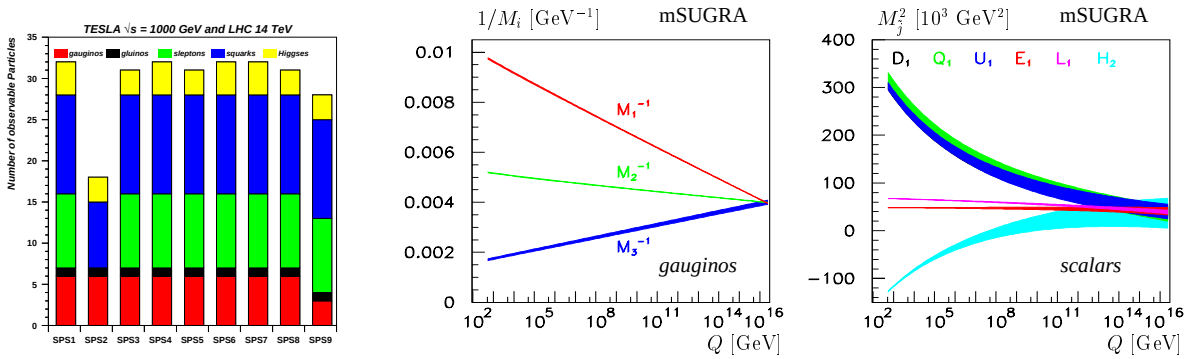

Figure 16: Making use of combined LC and LHC results. Accessible sparticles of SUSY spectra from Snowmass benchmarks [24] (left). Evolution, from low to high scales, of gaugino mass parameters (center) and first generation sfermion and Higgs H_2 mass parameters (right) of mSUGRA model SPS 1. Bands correspond to 1 st. dev. contours based on expected sparticle mass accuracies [25]

The proposed Linear Collider projects are planned to reach center-of-mass energies around 1 TeV, which should be sufficient to cover a large part of model predictions for sparticle masses. An extension to multi-TeV energies at a later stage may be required to detect and uncover the complete SUSY spectrum. It has been recognised by the international high energy physics community, that a high luminosity, TeV scale Linear Collider should be realised in the near future with high priority. Such a machine would beautifully complement the LHC searches with its preference for heavy coloured supersymmetric particles. It appears particularly attractive and most desirable that both hadron and lepton colliders take data at the same time and benefit mutually in their SUSY analyses from a combination of their results. For instance, the LC could provide the masses and quantum numbers of light gauginos and sleptons, while the LHC may

support information on the heavy squarks. Examples of such a synergy effect are presented in fig. 16. Almost all sparticles of the Snowmass benchmark spectra [7, 24] would be accessible and their properties could be determined. Using the accurate sparticle masses, it would be possible to establish in a model independent approach the nature of supersymmetry breaking [25]. The evolution of gaugino and scalar mass parameters to very high scales, shown for mSUGRA, clearly allows one to distinguish between models and to test unification. After a few years of e^+e^- Linear Collider operation a rich and coherent picture of supersymmetry could emerge.

Acknowledgement. I want to thank the organisers of SUSY 02 for the invitation to give this talk and for having prepared this excellent conference. I have profited from many stimulating discussions with my colleagues from the SUSY working group of the ECFA/DESY Study.

References

[1] T. Kamon, these proceedings

[2] F.E. Paige, these proceedings [hep-ph/0211017].

[3] TESLA Technical Design Report, DESY 2001-011, *Part II: The Accelerator; Part III: Physics at an e^+e^- Linear Collider* [hep-ph/0106315].

[4] American Linear Collider working group, SLAC-R-570, *Linear Collider physics resource book for Snowmass 2001, Part 2: Higgs and Supersymmetry studies* [hep-ex/0106056].

[5] ACFA Linear Collider working group report, KEK Report 2001-11, *Particle physics experiments at JLC* [hep-ph/0109166].

[6] CLIC Study Team, CERN 2000-008, *A 3 TeV e^+e^- linear collider based on CLIC technology*.

[7] B.C. Allanach et al., Eur. Phys. J. C 25 (2002) 113;
N. Ghodbane, H.-U. Martyn, hep-ph/0201233.

[8] H.-U. Martyn, G.A. Blair, Proc. *Physics and Experiments with Future Linear e^+e^- Colliders*, LCWS99, Sitges, Spain, 1999 [hep-ph/9910416];
H.-U. Martyn, Workshop *Physics at TeV Colliders*, Les Houches, France, 1999, hep-ph/0002290.

[9] P. Grannis, talk at LCWS02, Jeju Island, Korea, 2002, hep-ex/0211002;
M. Battaglia et al., hep-ph/0201177.

[10] W. Majerotto, these proceedings [hep-ph/0209137].

[11] J. Kalinowski, these proceedings.

[12] M. Dima et al, Phys. Rev. D 65 (2002) 71701.

[13] A. Freitas, A. v. Manteuffel, these proceedings [hep-ph/0211105];
A. Freitas et al., hep-ph/0211108.

[14] M.M. Nojiri, Phys. Rev. D 51 (1995) 6281;
M.M. Nojiri, K. Fujii, T. Tsukamoto, Phys. Rev. D 54 (1996) 6756.

[15] E. Boos et al., these proceedings [hep-ph/0211040].

[16] S.Y. Choi et al., Eur. Phys. J. C 22 (2001) 563 and Addendum ibid. C 23 (2002) 769.

[17] G. Moortgat-Pick, these proceedings [hep-ph/0211039].

[18] R. Keranen et al., Eur. Phys. J direct C 7 (2000) 1.

[19] H. Baer et al., Proc. *Physics and Experiments with Future Linear* e^+e^- *Colliders*, LCWS2000, Fermilab, USA, 2000

[20] D.K. Gosh et al., TESLA TDR, LC-TH-2000-051 [hep-ph/9904233].

[21] J. Gunion, S. Mrenna, Phys. Rev. D 64 (2001) 75002.

[22] S. Ambrosanio, G. Blair, Eur. Phys. J. C 12 (2000) 287.

[23] G.W. Wilson, Proc. *Physics and Experiments with Future Linear* e^+e^- *Colliders*, LCWS2000, Fermilab, USA, 2000

[24] N. Ghodbane, private communication.

[25] W. Porod, these proceedings [hep-ph/0210416];
G.A. Blair, W. Porod, P.M. Zerwas, hep-ph/021058.